*Desalination and Water Treatment*
www.deswater.com
doi: 10.5004/dwt.2023.29153

282 (2023) 127–138
January

# Adsorption of yttrium(III), neodymium(III), gadolinium(III), samarium(III), and lutetium(III) ions using 8-hydroxyquinoline intercalated bentonite

Mohamed S. Gaber*, Bahaa A. Salah, Abdelhakim T. Kandil

*Chemistry Department, Faculty of Science, Helwan University, Ain Helwan, Helwan 11795, Cairo, Egypt, emails: mohamed.Gaber@science.helwan.edu.eg (M.S. Gaber), BAHAA_HUSSEIN@science.helwan.edu.eg (B.A. Salah), Abdelhakimkandil@yahoo.com (A.T. Kandil)*

Received 28 July 2022; Accepted 28 November 2022

**ABSTRACT**

Due to the high cation exchange capacity, depressed permeability, low cost, and massive specific surface area, bentonite has crucial importance in the disposal of radioactive waste from their aqueous solutions. Here, the intercalation of 8-hydroxyquinoline onto the surface of Na-bentonite was carried out and the obtained material was used to explore the sorption conduct of lanthanides metal ions from their solutions. X-ray fluorescence, X-ray powder diffraction, Fourier-transform infrared spectroscopy, scanning electron microscopy, and transmission electron microscopy spectra were done to characterize unmodified and modified bentonite. The changes in the environmental parameters such as contact time, solution pH, sorbent mass, initial concentration, and temperature were optimized. Sorption isotherm was simulated by Langmuir and Freundlich equations and the outcomes revealed that the Langmuir model was appropriate for the sorption of lanthanides onto 8-hydroxyquinoline bentonite (HQ-bentonite) and the maximum sorption capacities values were found to be 26.1, 47.6, 32.6, 39.2, and 40.9 mg/g for $Y^{3+}$, $Nd^{3+}$, $Gd^{3+}$, $Sm^{3+}$, and $Lu^{3+}$, respectively, at 303 K. On the other hand, the regeneration studies were investigated with various reagents.

*Keywords:* Adsorption; Lanthanides; Bentonite; Intercalation; 8-hydroxyquinoline

## 1. Introduction

Lanthanide elements are vastly used in electronic devices, permanent magnet materials, microelement fertilizers, feed additives in agriculture, fluorescent materials, and MRI reagents in medicine [1]. Disposing of industrial or radioactive waste in an underground repository is extremely serious since this waste can dissolve in groundwater. As a result, the disposal of radioactive metal ions from junk water plays an indispensable role in effluent treatment [2]. Exposure to rare earth elements also fulfills adverse impacts on human health as pneumoconiosis in the lung, hepatotoxic and neurotoxic effects, histopathological system damage, the activity of various enzymes, and the activity of calcium channels in living organism cells, and even cancer [3]. The numerous sources of radioactive wastes include diverse industrial activities such as mining, nuclear armament, nuclear power plants, and processes producing nuclear fuels [4]. Several creative techniques such as flotation, solvent extraction [5], ion exchange [6], nanofiltration [7], chemical precipitation [8,9] membrane dialysis, adsorption [10], biological processes [11], and chromatographic extraction have been attempted to eject the hazardous pollutants from waste. Adsorption is rapid kinetics [12], inexpensive, easy operation, and simple selectivity [13] procedure that has become an effective process for eliminating radioactive metal ions from wastewater. Clay minerals, for instance, bentonite, are known

* Corresponding author.

to be highly efficient in the removal of radioactive metal ions because of their high adsorption capacity, abundance, and, low-cost [14]. The major structure of bentonite is one central alumina octahedral sheet ($AlO_6$) situated between two silica tetrahedral sheets ($S_iO_4$). The isomorphous substitution of Al(III) with Mg(II) and Si(VI) with Al(III) in the octahedral and tetrahedral layers, respectively; is the cause of the negative charge on the bentonite surface, which necessitates a charge balance between this negative charge and the exchangeable cations, such as ($Na^+$, $Ca^{2+}$, etc.), on the layer surfaces [15]. Bentonite has several merits, compared to other adsorbent materials. For instance, it has surface acidity, ubiquitous presence in most soils, accessibility, the crystallinity of its smectite, chemical composition, high surface area, low permeability, great cation exchange capacity, an intensive adsorptive affinity for inorganic and organic contaminants, and low-cost [3,16]. Since bentonite has a relatively low adsorption capacity, it can be modulated to promote its adsorption ability [17]. A complexing agent (8-hydroxyquinoline) which has a selective reactivity for the target metal ions was intercalated in bentonite [13]. It is known that modified Na-bentonite (HQ-bentonite) is a highly efficient adsorbent for the removal of heavy metal ions [13,18,19]. The present work aimed to modify Na-bentonite with 8-hydroxyquinoline and use the obtained material for the plucking out of lanthanides metal ions from their aqueous solutions. The changes in the environmental factors such as solution pH, contact time, sorbent mass, initial concentration, and temperature were optimized. Sorption isotherm models have been inspected in terms of Langmuir and Freundlich equations. Furthermore, desorption studies were performed using various eluting reagents.

## 2. Materials and methods

### 2.1. Reagents

Stock solution (1,000 mg/L) of target-ions were prepared by dissolving 1.27, 1.17, 1.16, 1.15, and 1.14 g, respectively of their oxides (Riedel-De Haen AG, Germany), in 10 mL of concentrated perchloric acid and the solution was evaporated to dryness. Then, 5 mL of the previous acid was added and the solution was diluted to volume with 0.1 N perchloric acid. It is a noteworthy fact that analytical-grade chemicals were used.

### 2.2. Adsorbent

The clay was purchased from Research-Lab Fine Chem Industries (Kalbadevi, India). The methylene blue procedure was used to estimate the cation exchange capacity [20], and it was found as 0.900 mmol/g. Regarding the reported process [19], natural clay was modified with an organic material (8-hydroxyquinoline) purchased from (Sigma-Aldrich, St. Louis, MO, USA, with 99% purity).

### 2.3. Samples characterization

The chemical compositions of the samples were defined by X-ray fluorescence (XRF; PANalytical Axios Advanced, The Netherlands). X-ray diffraction patterns of materials were obtained using the Bruker D8 Advance Diffractometer (Bruker AXS, Karlsruhe, Germany) with Cu-K$\alpha$ (K$\alpha$1 = 1.5406 Å). The range at which the 2$\theta$ value was scanned is from 2° to 70° with step size and time (0.02°) and (0.4 s), respectively. Scanning electron microscopy (SEM) images of the materials were characterized by using SEM-Quanta FEG-250 instrument (FEI Corporate, Hillsboro, OR, USA) at high accelerating voltage (30 kV); and at high magnification up to 100,000 X. High-resolution transmission electron microscope (JEOL JEM-2100, Japan) operating at 200 keV was used. The Fourier Transform Infrared spectra of the samples were carried out by Spectrum Two Perkin Elmer Fourier-transform infrared spectroscopy (FTIR) analyzer (PerkinElmer Inc., Waltham, MA, USA), over spectral vibration range from 400 to 4,000 $cm^{-1}$ using the ATR method. pH values were recorded using a pH meter (Jenco 6173, Shanghai, China). The spectra absorption was measured using a UV-Vis spectrophotometer (Jasco V-630, Tokyo, Japan).

### 2.4. Experimental methods

The sorption of trivalent lanthanides ions ($Ln^{3+}$) onto the modified clay was determined by a batch equilibration procedure in which 0.1 g HQ-bentonite was suspended in 50 mL solution of all the tested metal ions at various experimental circumstances and pH ranges (2–7) ± 0.1 (adjusted by adding measly volumes of 0.1 mol/L NaOH and 0.1 mol/L $HClO_4$). At equilibrium, the content was centrifuged for 10 min at 4,000 rpm and the Arsenazo(III) procedure with a spectrophotometer at 650 nm was utilized to determine the residual concentrations of lanthanides metal ions [21]. The amount of adsorbate taken up by the sorbent material was measured from the variance between the initial and equilibrium concentration. The sorption amount ($q_e$, mg/g) of metal ions taken up by HQ-bentonite was estimated using Eq. (1):

$$q_e = \left(C_0 - C_e\right)\frac{\nu}{m} \tag{1}$$

where $q_e$ is the adsorption capacity of the modified clay (mg/g); $C_o$ and $C_e$ are the metal ions concentrations in the initial and equilibrium solution (mg/L), respectively; $V$ is the volume of aqueous solution (L) and $m$ is the mass of sorbent (g).

The sorption percentage (%) values were found from the following equation:

$$\text{Sorption}\left(\%\right) = \frac{C_0 - C_e}{C_e} \times 100 \tag{2}$$

### 2.5. Desorption studies

From the regeneration point of view, the steadiness of the adsorbent is critical and the adsorbed metal ions should be easily desorbed without the destruction of the adsorbent under the operating circumstances. Desorption studies were carried out using three eluting reagents: NaCl, $HNO_3$, and HCl with various concentrations (0.05–0.25 M) to eliminate

metal ions and to determine the desorption properties of HQ-bentonite. 0.1 g of the bound metal ion was shaken with 50 mL of the stripping agent at room temperature. The stripping percentage was determined by the following equation:

$$\text{Striping}(\%) = \frac{C}{C_o} \times 100 \quad (3)$$

where $C_o$ and $C$ are the metal ions concentrations accumulated on the adsorbent surface and suspended in the eluting agent after a proper time (mg/L), respectively.

## 3. Results and discussion

### 3.1. Samples characterization

#### 3.1.1. Chemical constituents of natural and modified bentonite

Table 1 shows the chemical composition of unmodified and modified clay. The master components of the materials are $SiO_2$ and $Al_2O_3$ along with traces of K, Fe, Ti, Mg, and Ca oxides [13]. After the modulation of Na-bentonite the mass % of $Na_2O$ decreases due to the exchange of the sodium ions of the natural clay mineral with 8-hydroxyquinoline.

#### 3.1.2. X-ray powder diffraction analysis

Fig. 1 demonstrates the X-ray powder diffraction (XRD) diagram of sodium bentonite and HQ-bentonite. The basal spaces of the former and latter were observed at 12.953 and 15.857 Å, respectively. The value of $d_{001}$ of sodium bentonite expanded by 2.904 Å. This referred that the organic material (8-hydroxyquinoline) being immobilized in the interior layers of the pure bentonite [13].

#### 3.1.3. SEM micrographs and energy-dispersive X-ray spectroscopy analysis

SEM micrograph images of Na-bentonite, HQ-bentonite, Y(III), Nd(III), Gd(III), Sm(III), and Lu(III) ions loaded modified bentonite are presented in Figs. 2–7. Results demonstrated that the surface microstructure of sodium bentonite was spongier and relatively smoother than HQ-bentonite which became inflated by a few holes after the modification. This confirmed the intercalation of the chelating species in the interlayer space of the sodium bentonite.

Table 1
Chemical components of natural and modified clay

| Constituents | Mass% | |
|---|---|---|
| | Natural clay | Modified clay |
| $Na_2O$ | 4.616 | 0.504 |
| $SiO_2$ | 46.75 | 44.57 |
| $Al_2O_3$ | 19.86 | 17.86 |
| $Fe_2O_3^{tot}$ | 12.23 | 11.74 |
| MgO | 1.947 | 1.515 |
| CaO | 1.019 | 0.311 |
| $TiO_2$ | 2.152 | 2.017 |
| $P_2O_5$ | 0.123 | 0.089 |
| $K_2O$ | 1.055 | 0.934 |
| $SO_3$ | 0.289 | 0.033 |
| Loss on ignition (LOI) | 8.700 | 19.70 |

#### 3.1.4. Transmission electron microscopy images

For further confirmation, in Fig. 8, a transmission electron microscopy (TEM) image of a selected sample of the modified bentonite is compared with those of the parent. As is observed, the crystalline-layered structure of the pure bentonite is clear in micrograph (a). Conversely, 8-hydroxyquinoline crystallites were formed on the surface of the clay as shown in micrograph (b).

#### 3.1.5. FTIR analysis

FTIR patterns of the natural bentonite, the modified bentonite, $Y^{3+}$, $Nd^{3+}$, $Gd^{3+}$, $Sm^{3+}$ and $Lu^{3+}$ ions loaded 8-hydroxyquinoline-bentonite, respectively are shown in Fig. 9a–g. The confirmation of the intercalation of the 8-hydroxyquinoline onto the natural clay and the interactive nature of the modified clay with metal ions will be demonstrated. The absorption peak at 3,620 $cm^{-1}$ in Fig. 9a is referred to as the (O–H) stretching vibration of the (Si–OH) group. The intensive band at 1,000 $cm^{-1}$ is attributed to the (Si–O–Si) groups of the tetrahedral sheet. The stretching vibration of (Al–Al–OH) showed a strong peak at 912 $cm^{-1}$. Likewise, the quartz in the sample formed a band at 798 $cm^{-1}$. In addition, the deformation and bending modes of the Si–O bond created a stretching vibration band at 693 $cm^{-1}$. The peaks at 466 and 524 $cm^{-1}$ are ascribed to (Si–O–Si) and (Al–O–Si) bending vibrations, respectively. The modified bentonite spectrum (Fig. 9b) revealed various peaks which are not observed in the natural bentonite such as C–C and C–N ring stretching vibrations which formed at 1,604; 1,500; 1,466; 1,381 and 1,322 $cm^{-1}$. Furthermore, the ring bending vibration formed at 825 $cm^{-1}$ [13]. This proved the intercalation of 8-hydroxyquinoline onto the pure bentonite. The adsorption of the target metal ions onto HQ-bentonite led to a shift in different peaks such as the (O–H) stretching vibration of the silanol (Si–OH) group which was shifted to 3,621 $cm^{-1}$ for all the metal ions as shown in Fig. 9c–g. The C–C and C–N ring stretching bands were moved at 1,637; 1,500; 1,466; 1,381 and 1,319 for Y(III); 1,634; 1,500; 1,466; 1,381 and 1,320 $cm^{-1}$ for Nd(III); 1,637; 1,499; 1,466; 1,380 and 1,318 $cm^{-1}$ for Gd(III); 1,634; 1,500; 1,466; 1,381 and 1,318 $cm^{-1}$ for Sm(III); 1,634; 1,500; 1,467; 1,380 and 1,319 $cm^{-1}$ for Lu(III), whereas, the ring bending vibration was moved to 826 $cm^{-1}$ for Y(III); 825 $cm^{-1}$ for Nd(III), Gd(III), Sm(III) and Lu(III). The (Si–O–Si) bond of the tetrahedral sheet was shifted to 1,001 $cm^{-1}$ for Y(III); 999 $cm^{-1}$ for Nd(III); 1,002 $cm^{-1}$ for Gd(III); 1,000 $cm^{-1}$ for Sm(III) and 1,004 $cm^{-1}$ for Lu(III). The stretching vibration of (Al–Al–OH) was moved to 913 $cm^{-1}$ for Gd(III) and Lu(III); 912 $cm^{-1}$ for Y(III), Nd(III), and Sm(III). The deformation and bending bands of the (Si–O) bond were moved to 693 $cm^{-1}$ for Lu(III); 692 $cm^{-1}$ for Y(III), Nd(III), Gd(III), and Sm(III). The bending vibrations band of (Si–O–Si) was moved to 467 $cm^{-1}$ for Nd(III); 466 $cm^{-1}$ for Y(III), Gd(III), and Lu(III); 464 $cm^{-1}$ for Sm(III), whereas, the (Al–O–Si)

was moved to 523 $cm^{-1}$ for Y(III), Gd(III), Sm(III) and Lu(III); 519 $cm^{-1}$ for Nd(III). These shifts confirm the interaction between lanthanides and the modified bentonite.

### 3.1.6. Influence of time

Contact time plays a pivotal role in the optimization processing period. The influence of shaking time on the sorption of lanthanides onto HQ-bentonite has been demonstrated in Fig. 10. The results indicated that the uptake percentage of lanthanides ions increases dramatically with increasing the contact time till reaches the equilibrium at 5 min and then remained constant.

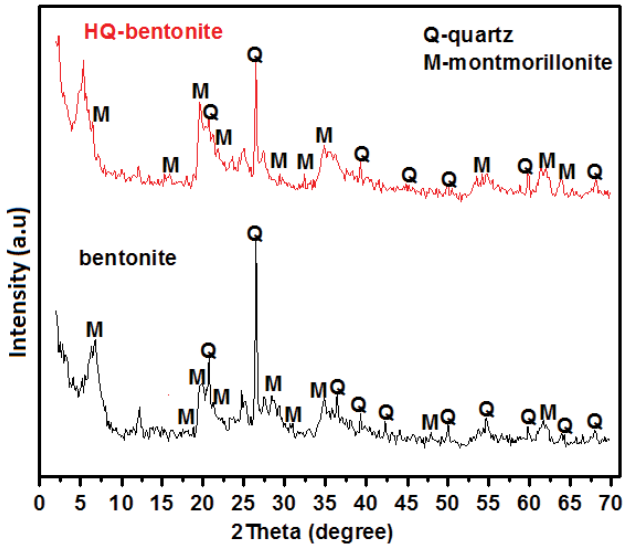


Fig. 1. X-ray powder diffraction patterns of pure and modified clay.

### 3.1.7. Influence of solution pH

Unquestionably, the pH of the solution is an extremely significant factor that impacts the sorption of metal ions. It is observed that at pH values (2–7); the modified bentonite exhibits a negative surface charge and a negative zeta potential. In addition, it has no point of zero charges ($pH_{pzc}$) [13]. Fig. 11 demonstrates the impact of initial pH on lanthanides' sorption onto the modified bentonite. The results demonstrated that the uptake percentage climbs with the rise of pH to a maximum value of pH 6 ± 0.1. In more precisely, it was observed that the precipitate formed above pH 6. This is due to the hydrolysis of $Ln^{3+}$ occurring at pH as low as 6 and different species can be formed, such as $Ln(OH)^{2+}$, $Ln(OH)_2^+$, $Ln(OH)_3$, $Ln(OH)_4$ [22]. Moreover, reduced absorption of rare earth elements (REEs) at lower pH values is more realistic due to the protonation of the active sites in HQ-bentonite, which blocks its binding efficiency towards the REEs. Additionally, the positive charge of the surface declines with increasing pH, which would result in lower Columbia repulsion of the adsorbed rare earth element. Consequently, due to lanthanides precipitation appearing at pH 7, pH 5 was utilized for further experiments.

### 3.1.8. Influence of metal ions concentration

Fig. 12 illustrates the impact of the initial concentration of lanthanides on the uptake proportion of the modified bentonite. The results revealed that the rate of adsorption declined dramatically with the increase of the initial

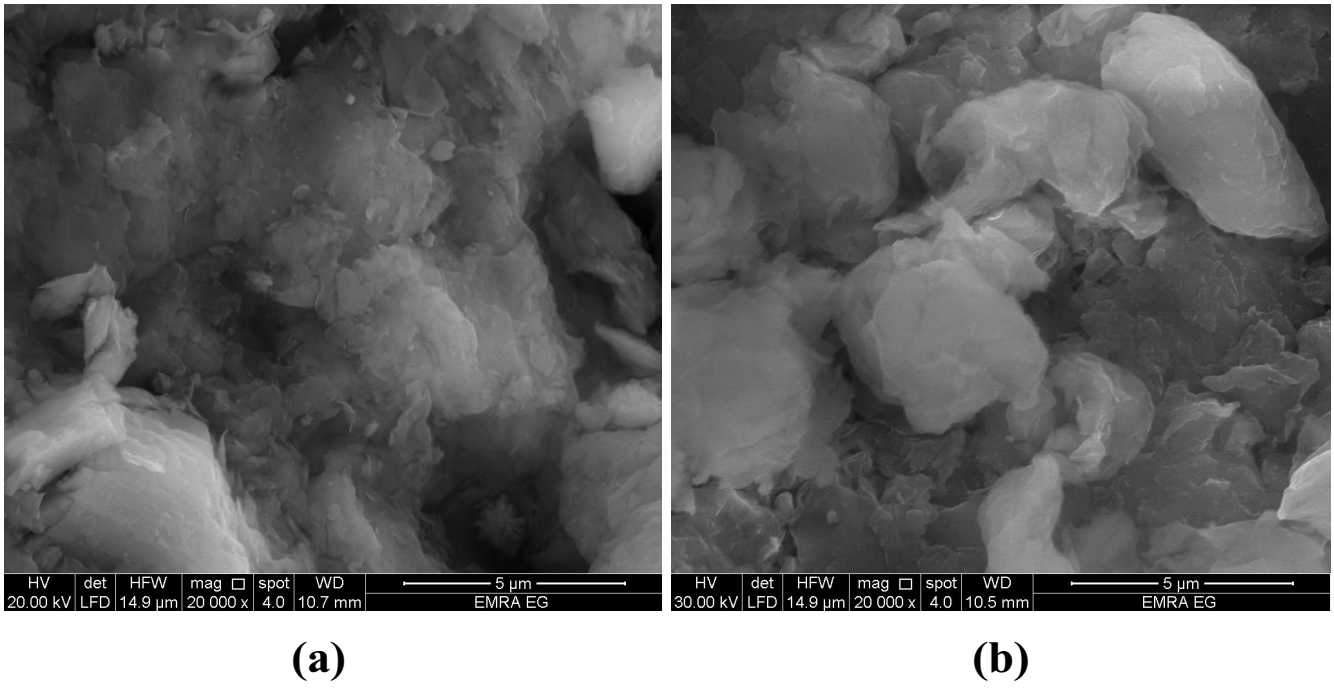


Fig. 2. SEM micrographs of (a) pure bentonite and (b) modified bentonite.

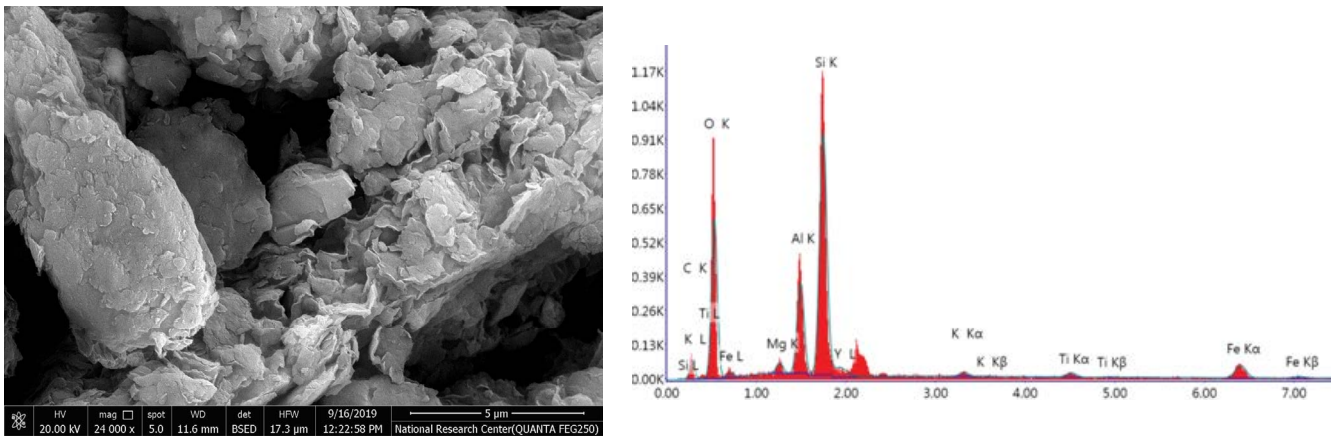


Fig. 3. SEM micrographs and energy-dispersive X-ray spectroscopy (EDS) analysis of Y(III) loaded modified bentonite.

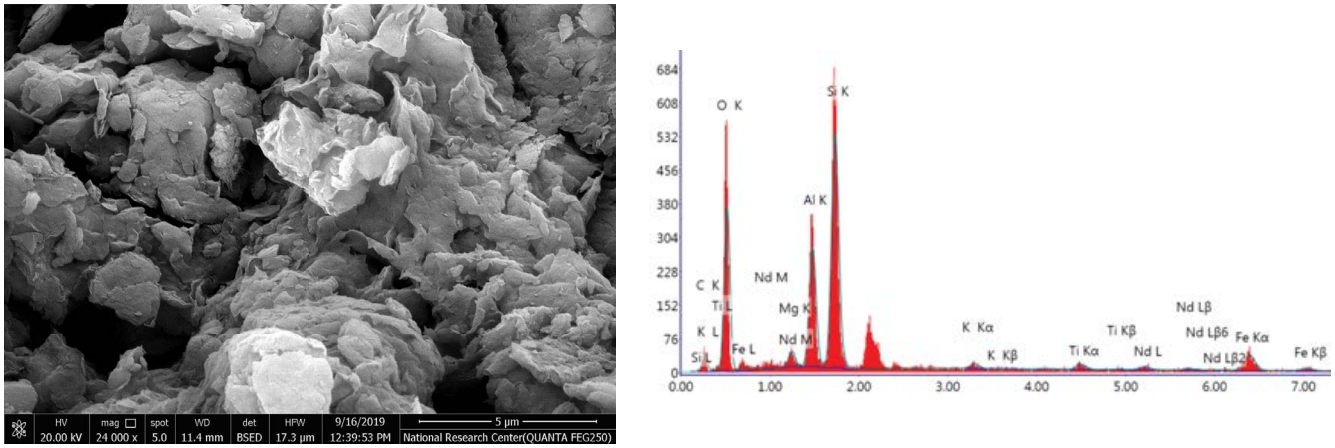


Fig. 4. SEM micrographs and EDS analysis of Nd(III) loaded modified bentonite.

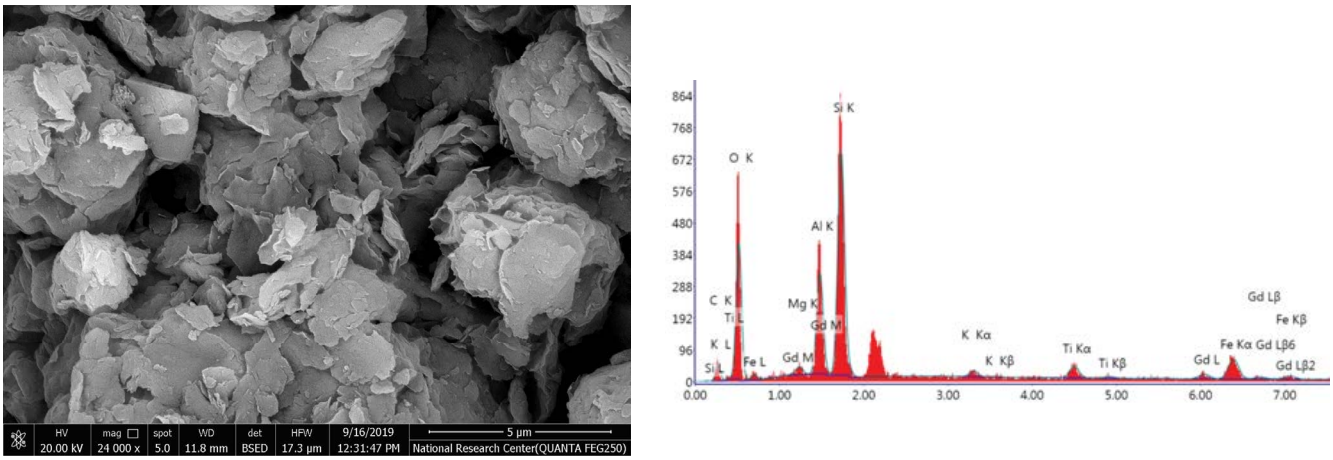


Fig. 5. SEM micrographs and EDS analysis of Gd(III) loaded modified bentonite.

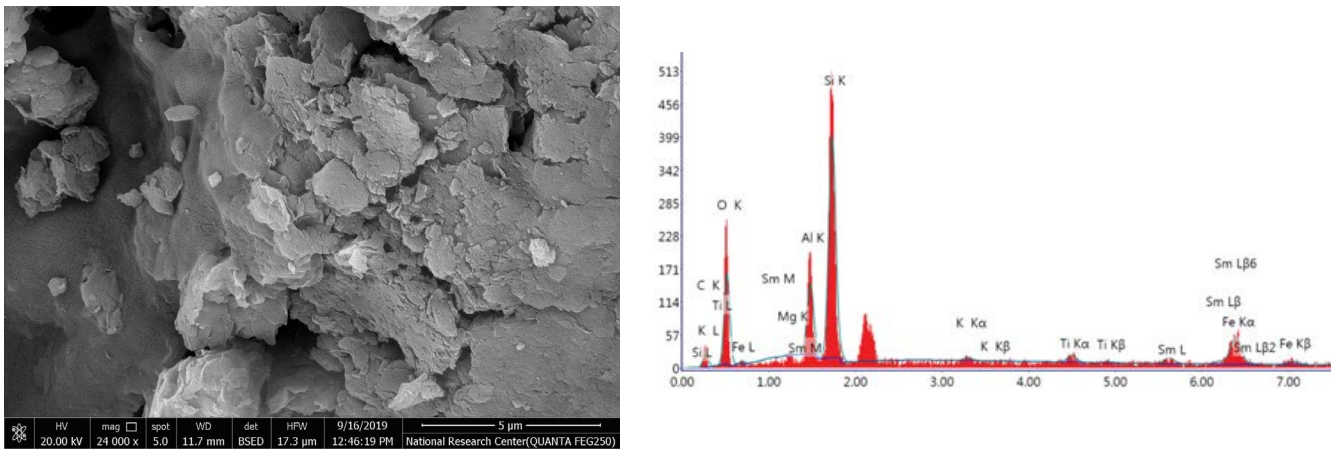


Fig. 6. SEM micrographs and EDS analysis of Sm(III) loaded modified bentonite.

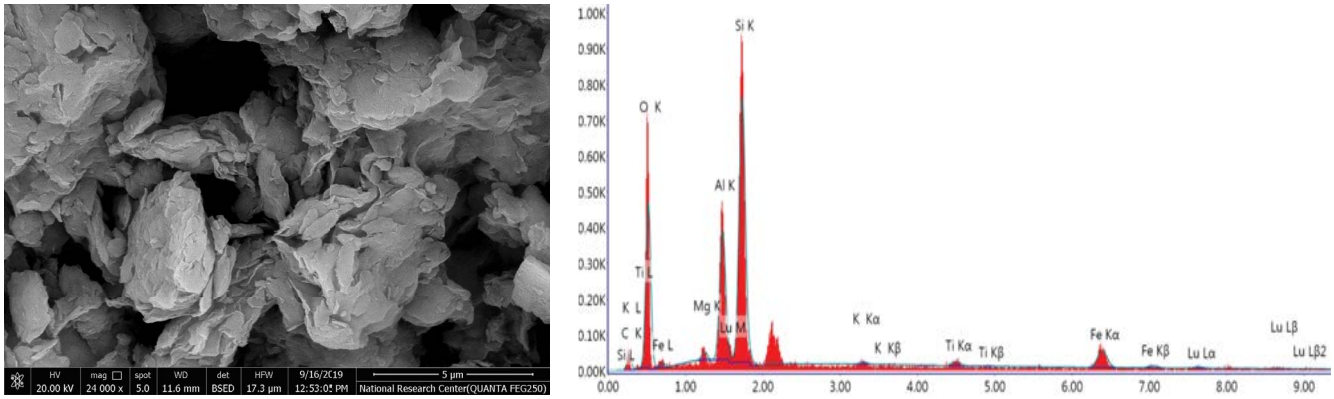


Fig. 7. SEM micrographs and EDS analysis of Lu(III) loaded modified bentonite.

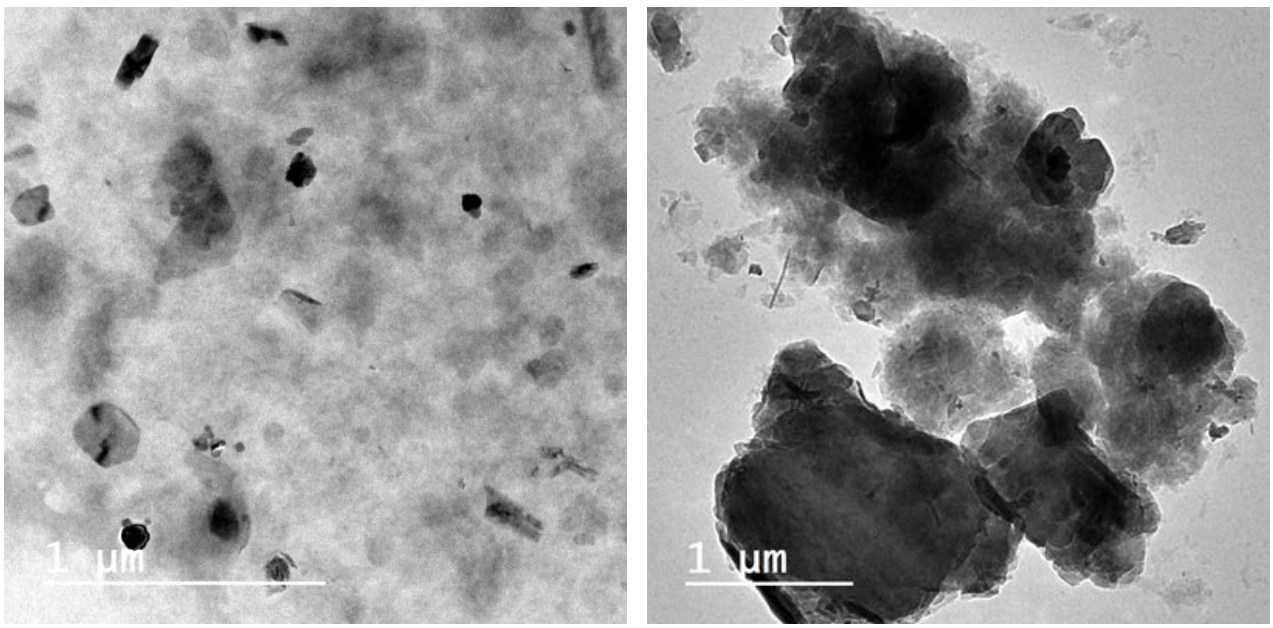


Fig. 8. TEM images of (a) pure bentonite and (b) modified bentonite.

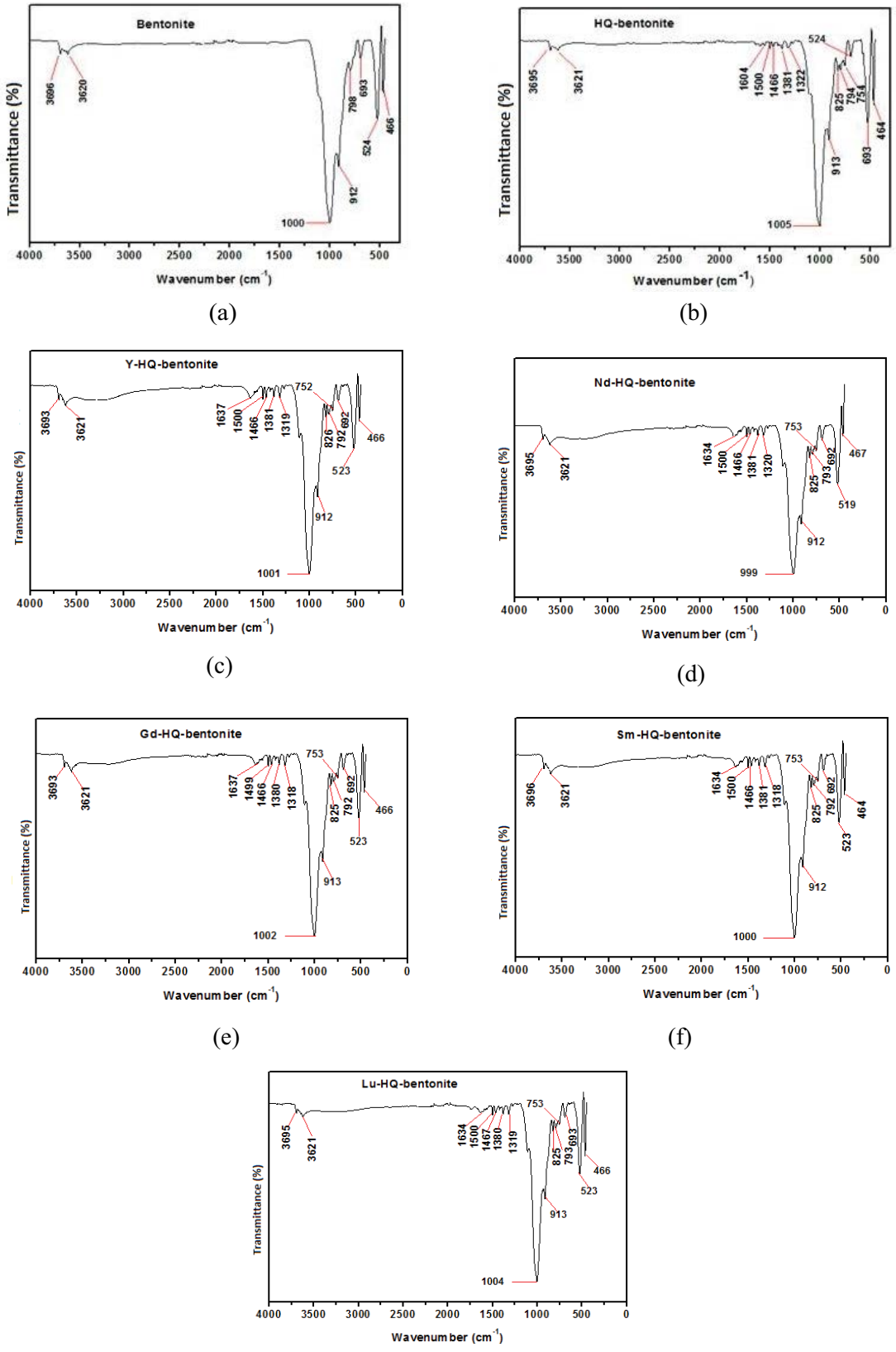


Fig. 9. FTIR spectra of (a) pure bentonite, (b) modified bentonite, (c) Y(III) loaded modified bentonite, (d) Nd(III) loaded modified bentonite, (e) Gd(III) loaded modified bentonite, (f) Sm(III) loaded modified bentonite and (g) Lu(III) loaded modified bentonite.

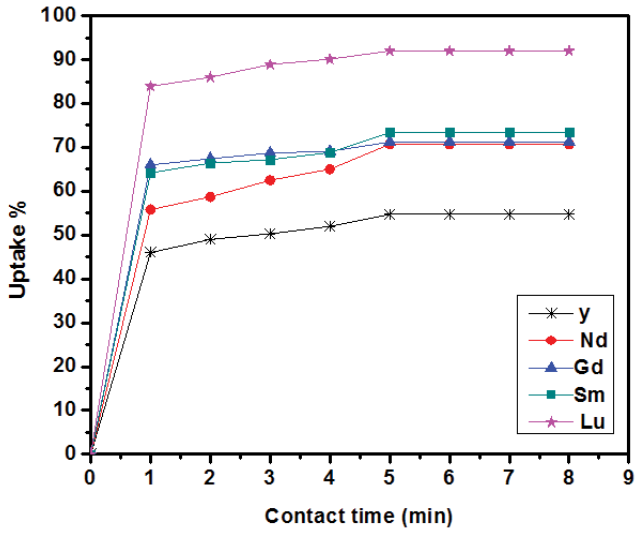


Fig. 10. Impact of contact time on Y(III), Nd(III), Gd(III), Sm(III), and Lu(III) ions adsorption onto modified bentonite. Experimental conditions: 0.1 g modified bentonite; 50 mL aqueous solution; 100 mg/L metal ion; pH 5; temperature 303 K.

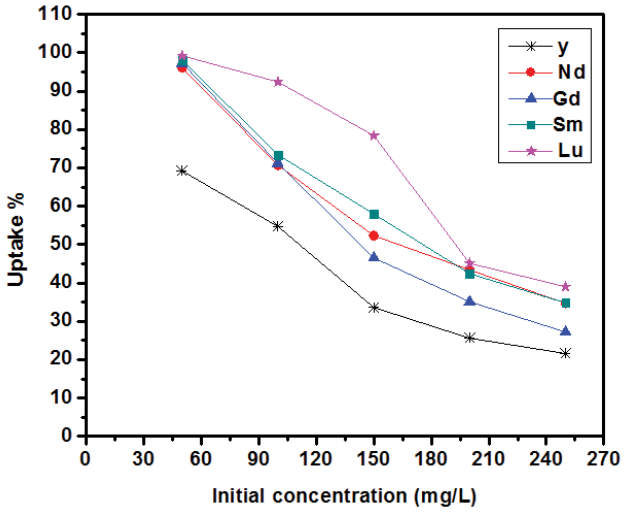


Fig. 12. Impact of metal ion's initial concentration on Y(III), Nd(III), Gd(III), Sm(III), and Lu(III) ions adsorption onto modified bentonite. Experimental conditions: 0.1 g modified bentonite; 50 mL aqueous solution; pH 5; contact time 5 min; temperature 303 K.

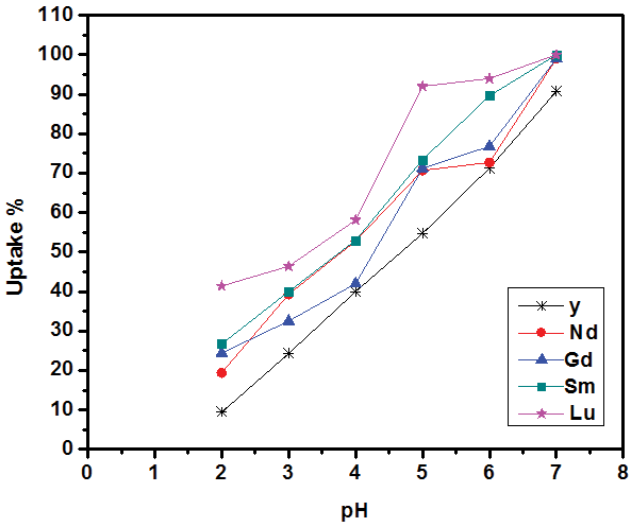


Fig. 11. Impact of pH on $Y^{3+}$, $Nd^{3+}$, $Gd^{3+}$, $Sm^{3+}$, and $Lu^{3+}$ ions adsorption onto modified bentonite. Experimental conditions: 0.1 g modified bentonite; 50 mL aqueous solution; 100 mg/L metal ion; contact time 5 min; temperature 303 K.

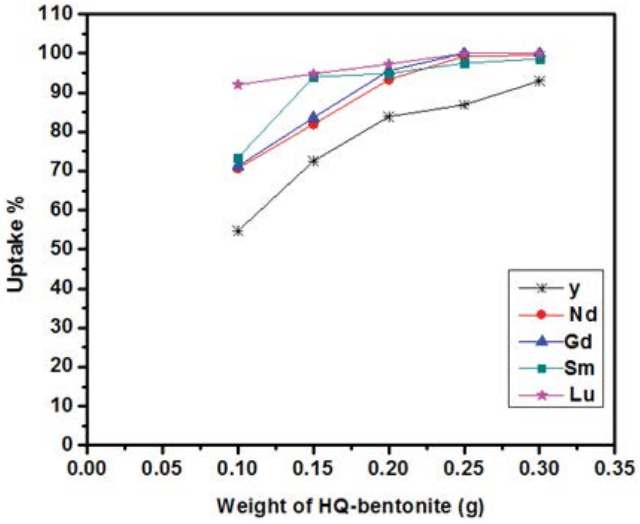


Fig. 13. Impact of adsorbent mass on $Y^{3+}$, $Nd^{3+}$, $Gd^{3+}$, $Sm^{3+}$, and $Lu^{3+}$ ions adsorption onto modified bentonite. Experimental conditions: 100 mg/L metal ion; 50 mL aqueous solution; pH 5; contact time 5 min; temperature 303 K

concentration of metal ions. This is due to the higher percentage of sorption quantity of metal ions on the modified bentonite surface to the available void sites.

### 3.1.9. Influence of sorbent dosage

Fig. 13 shows the impact of the sorbent mass on the adsorption of lanthanides onto the modified bentonite. Undoubtedly, as the amount of sorbent material in the solution soar, the number of its particles upsurges. Consequently, the accumulation of metal ions on its surface increases which enhances the interaction between the metal ions and binding sites.

### 3.1.10. Influence of temperature

The effect of temperature on the sorption of lanthanides metal ions onto the modified bentonite was conducted by contacting 0.1 g of HQ-bentonite with a 150 mg/L of metal ion suspended in 50 mL aqueous solution, adjusted at pH 5, and shaken for 5 min at various temperatures (from 303 to 333 K). It was observed that the uptake ratio of all

tested metal ions witnessed a constant rate with increasing temperatures.

### 3.2. Sorption isotherms

Different sorption isotherm models can be used for analyzing adsorption equilibrium data. Here, the adsorption equilibrium data were characterized using the Langmuir and Freundlich isotherm models.

#### 3.2.1. Freundlich isotherm

The Freundlich model supposes that the sorption occurs at specific heterogeneous active sites and there is an interaction between the adsorbed species. In addition, the model can be applied to multilayer sorption. The Freundlich equation can be clarified by the linearized equation [23].

$$\log q_e = \log k + \frac{1}{n}\log C_e \tag{4}$$

where $C_e$ (mg/L) and $q_e$ (mg/g) are the equilibrium concentrations of metal ions in solution and on the adsorbent material, respectively. $k$ and $n$ are Freundlich constants (L/mg) which are indicators of sorption capacity and sorption intensity, respectively. $1/n$, and log$k$ are the slope and intercept, respectively; of the straight line resulting from the plot of log$q_e$ against log$C_e$. Freundlich isotherm parameters are presented in Table 2. The value of $n$ indicates the type of adsorption, where if the value of $n = 1$ the sorption is a chemical process [4]. Table 2, shows that the values of $n$ for the target metal ions are above unity. As a result, the adsorption of lanthanides metal ions onto the modified bentonite is a physical process. Additionally, the values of $R^2$ indicated that the Freundlich isotherm model does not fit the sorption of lanthanides metal ions onto the modified bentonite.

#### 3.2.2. Langmuir isotherm

Langmuir isotherm model is adequate for homogeneous surface energy frameworks. It is based on the hypothesis that only a saturated monolayer of adsorbates is shaped without interaction among them.

Langmuir equation can be defined by the linearized equation [23].

$$\frac{C_e}{q_e} = \frac{1}{bQ_e} + \frac{C_e}{Q_e} \tag{5}$$

where $C_e$ (mg/L) and $q_e$ (mg/g) are the equilibrium concentrations of metal ions in solution and on the adsorbent material, respectively. $Q_e$ (mg/g) is the maximum removal capacity and $b$ (L/mg) is a constant referred to as the heat of sorption. $1/Q_e$ and $1/bQ_e$ are the slope and the intercept, respectively; of the regression line resulting from the plot of $C_e/q_e$ vs. $C_e$ as shown in Fig. 14. Table 2 showed the Langmuir isotherm parameters with correlation coefficients. Eq. (6) was utilized to calculate the Langmuir equilibrium parameter $R_L$ [23].

$$R_L = \frac{1}{\left(1 + bC_0\right)} \tag{6}$$

where $C_o$ (mg/L) is the standard concentration of metal ions, $b$ (L/mg) is a constant referred to as the heat of sorption. The adsorption isotherm nature is determined using the

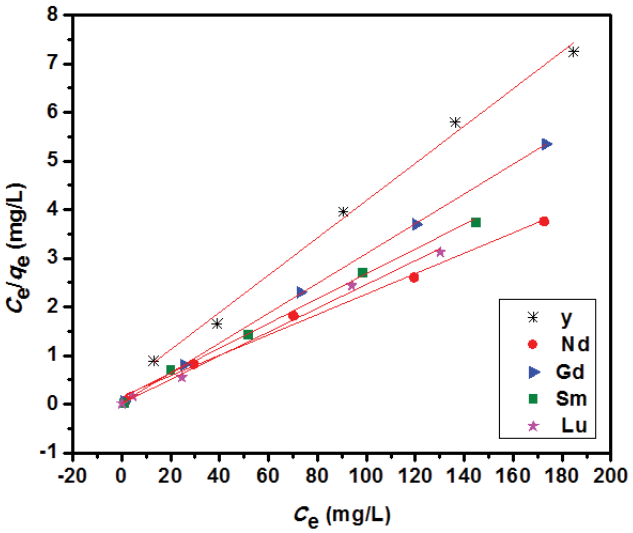


Fig. 14. Langmuir sorption isotherm of lanthanides adsorption onto modified bentonite. Experimental conditions: 0.1 g modified bentonite; 50 mL aqueous solution; pH 5; contact time 5 min.; temperature 303 K.

Table 2
Isotherm constants parameters and values of linear correlation factors ($R^2$) for the sorption of lanthanides metal ions onto modified bentonite

| Metal ion | Freundlich isotherm | | | Langmuir isotherm | | |
|---|---|---|---|---|---|---|
| | $N$ | log$K$ | $R^2$ | $Q_e$ (mg/g) | $b$ (L/mg) | $R^2$ |
| Y(III) | 5.5 | 1.00446 | 0.70 | 26.1 | 0.108 | 0.994 |
| Nd(III) | 6.2 | 1.30888 | 0.983 | 47.6 | 0.126 | 0.991 |
| Gd(III) | 9.9 | 1.30934 | 0.883 | 32.6 | 0.959 | 0.999 |
| Sm(III) | 5.6 | 1.21049 | 0.986 | 39.2 | 0.195 | 0.996 |
| Lu(III) | 4.5 | 1.21403 | 0.857 | 40.9 | 1.187 | 0.996 |

value of the Langmuir equilibrium parameter to be favorable ($0 < R_L < 1$), unfavorable ($R_L > 1$), linear ($R_L = 1$), or irreversible ($R_L = 0$) [24]. Calculated data indicated that the $R_L$ value was found to be 0.038, 0.03, 0.004, 0.023, and 0.0004 for Y(III), Nd(III), Gd(III), Sm(III), and Lu(III) ions, respectively, this reveals that the adsorption of the lanthanides metal ions onto the modified bentonite is favorable.

### 3.3. Desorption analysis

Undoubtedly, desorption is one of the most essential aspects of the applicability of the adsorbents [25]. Fig. 15 demonstrates the higher striping percentage using HCl and $HNO_3$ compared with NaCl, also as the concentrations of striping agents increased, the striping percentage increased.

### 3.4. Comparison with the other sorbent materials

Table 3 compares the efficiency of the HQ-bentonite adsorbent with other materials. It was obvious that the sorption capacity of the modified bentonite was greater than the sorption capacity of the other sorbent materials listed. As a result, HQ-bentonite has a higher potential for the removal of Y(III), Nd(III), Gd(III), Sm(III), and Lu(III) from their aqueous solutions.

## 4. Conclusions

In this paper, the modification of Na-bentonite by 8-hydroxyquinoline was done. SEM, TEM, XRF, FTIR, and XRD patterns were carried out to characterize the surface microstructure, chemical constituents, and functional groups of unmodified and modified bentonite. The batch procedure was used to explore the adsorption of lanthanides metal ions from their aqueous solutions onto modified bentonite under the effect of several parameters like contact time, solution pH, sorbent mass, temperature, and initial concentration. Adsorption equilibrium data were analyzed using Langmuir and Freundlich sorption isotherm models, the results demonstrated that the adsorption of lanthanides metal ions onto modified bentonite was better fitted to the Langmuir adsorption isotherm than the Freundlich model and the maximum sorption capacities values were found to be 26.1, 47.6, 32.6, 39.2 and 40.9 mg/g for Y(III), Nd(III), Gd(III), Sm(III) and Lu(III), respectively, at 303 K. The experimental results confirmed that 0.25 M $HNO_3$ or HCl are successful reagents for the regeneration of the sorbent material after the elution of lanthanides metal ions. It is essential to regenerate the sorption material after capturing the metal ions due to it allows the materials to be used cost-effectively, especially in field applications. The current work has revealed the value of the modified bentonite as an effective sorbent material for eliminating radioactive metal ions from contaminated water.

## Declarations

### Ethical approval

Not applicable.

### Competing interests

The authors declare that they have no competing interests.

### Author's contributions

This work is part of the M.Sc. studies of the first author mentioned in the authors' list, Mohamed S. Gaber, under the supervision of the second author, B.A.S.; and the third author, A.T.K. B.A.S. and A.T.K have suggested the study plan and participated in the interpretation of the data and discussion of the results. Mohamed S. Gaber has done the experimental work, participated in the discussion of the results, and written and revised the manuscript.

### Funding

This work has not received any financial support.

Table 3
Comparison between the maximum sorption capacities of lanthanide elements onto various sorbents at room temperature

| Sorbent materials | Metal ions | $Q_{max}$ (mg/g) | References |
|---|---|---|---|
| Nano-thorium(IV) oxide | Y(III) | 10.5 | [26] |
| Nano-zirconium(IV) oxide | Y(III) | 18.0 | [26] |
| Nitrolite | Nd(III) | 4.13 | [27] |
| Kaolinite | Nd(III) | 0.576 | [28] |
| Dicyclohexano crown ether (DCHCE) | Gd(III) | 1.83 | [29] |
| Dibenzo crown ether (DBCE) | Gd(III) | 2.02 | [29] |
| Dimethacrylate–methacrylic acid copolymers | Gd(III) | 19.4 | [30] |
| Organomodified bentonite (BT-NHED) | Sm(III) | 17.7 | [31] |
| Nano-zirconium oxide | Sm(III) | 21.3 | [32] |
| 8-hydroxyquinoline bentonite (HQ-bentonite) | Y(III) | 26.1 | This work |
| | Nd(III) | 47.6 | |
| | Gd(III) | 32.6 | |
| | Sm(III) | 39.2 | |
| | Lu(III) | 40.9 | |

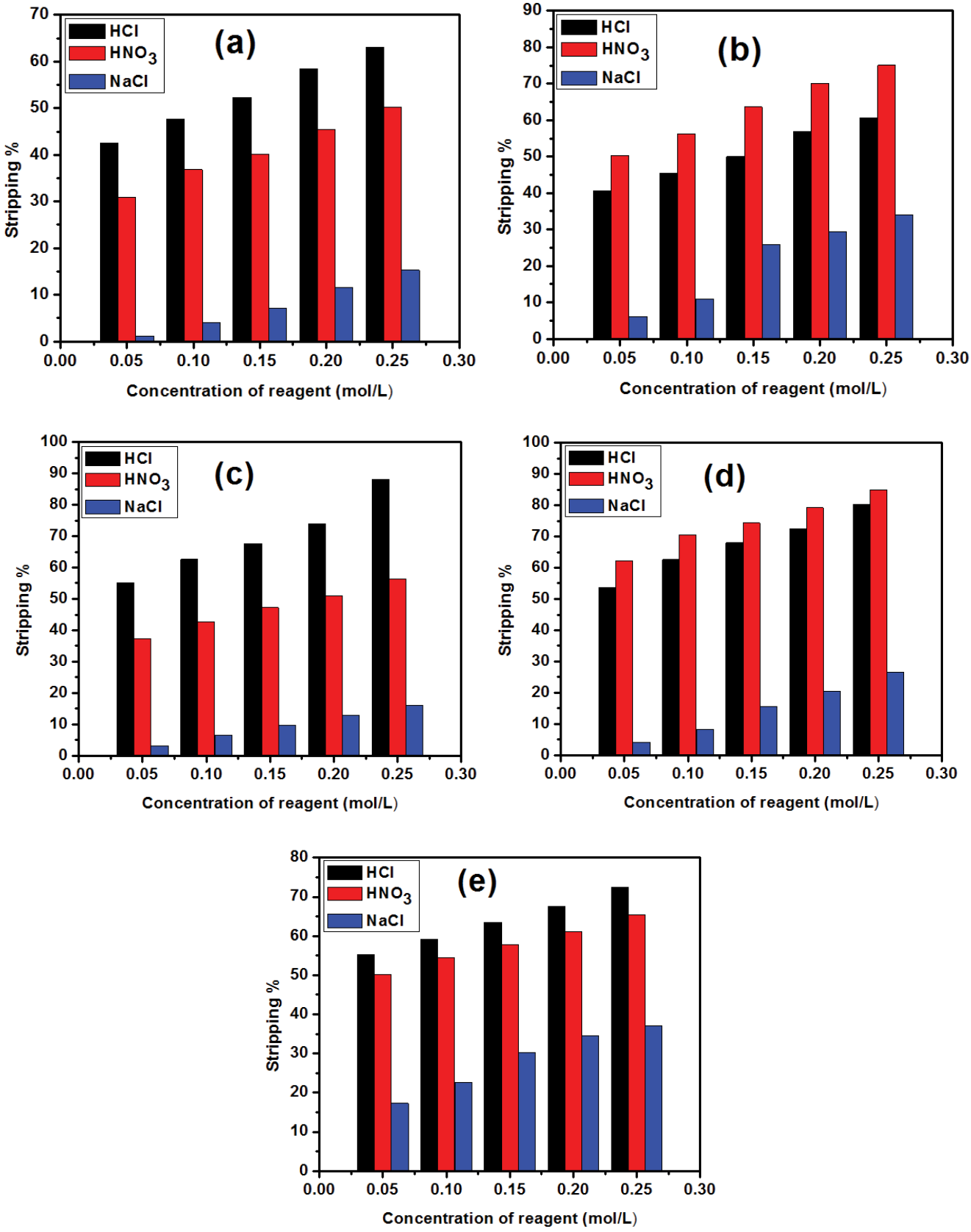


Fig. 15. Impact of NaCl, HCl, and $HNO_3$ on stripping proportion of (a) $Y^{3+}$, (b) $Nd^{3+}$, (c) $Gd^{3+}$, (d) $Sm^{3+}$, and (e) $Lu^{3+}$ from modified bentonite.

## Availability of data and materials

The present work findings have not been published before. Data and materials are all in the main text, figures, and tables.

## References


[1] J. Wang, Adsorption of aqueous neodymium, europium, gadolinium, terbium, and yttrium ions onto nZVI-montmorillonite : kinetics, thermodynamic mechanism, and the influence of coexisting ions, Environ. Sci. Pollut. Res., 25 (2018) 33521–33537.

[2] M.J. Kang, P.S. Hahn, Adsorption behavior of aqueous europium on kaolinite under various disposal conditions, Korean J. Chem. Eng., 21 (2004) 419–420.

[3] J. Xiao, Y. Chen, W. Zhao, J. Xu, Sorption behavior of U(VI) onto Chinese bentonite: effect of pH, ionic strength, temperature and humic acid, J. Mol. Liq., 188 (2013) 178–185.

[4] S.I.Y. Salameh, F.I. Khalili, A.H. Al-Dujaili, Removal of U(VI) and Th(IV) from aqueous solutions by organically modified diatomaceous earth: evaluation of equilibrium, kinetic and thermodynamic data, Int. J. Miner. Process., 168 (2017) 9–18.

[5] M.A. Bayyari, M.K. Nazal, F.A. Khalili, The effect of ionic strength on the extraction of thorium(IV) from nitrate solution by didodecylphosphoric acid (HDDPA), J. Saudi Chem. Soc., 14 (2010) 311–315.

[6] F. Houhoune, D. Nibou, S. Chegrouche, S. Menacer, Behaviour of modified hexadecyltrimethylammonium bromide bentonite toward uranium species, J. Environ. Chem. Eng., 4 (2016) 3459–3467.

[7] A. Favre-Réguillon, G. Lebuzit, D. Murat, J. Foos, C. Mansour, M. Draye, Selective removal of dissolved uranium in drinking water by nanofiltration, Water Res., 42 (2008) 1160–1166.

[8] A. Mellah, S. Chegrouche, M. Barkat, The precipitation of ammonium uranyl carbonate (AUC): thermodynamic and kinetic investigations, Hydrometallurgy, 85 (2007) 163–171.

[9] V. Tyrpekl, M. Beliš, T. Wangle, J. Vleugels, M. Verwerft, Alterations of thorium oxalate morphology by changing elementary precipitation conditions, J. Nucl. Mater., 493 (2017) 255–263.

[10] S. Aytas, M. Yurtlu, R. Donat, Adsorption characteristic of U(VI) ion onto thermally activated bentonite, J. Hazard. Mater., 172 (2009) 667–674.

[11] M.K. Sureshkumar, D. Das, M.B. Mallia, P.C. Gupta, Adsorption of uranium from aqueous solution using chitosan-tripolyphosphate (CTPP) beads, J. Hazard. Mater., 184 (2010) 65–72.

[12] Y.Q. Wang, Z. Bin Zhang, Q. Li, Y.H. Liu, Adsorption of uranium from aqueous solution using HDTMA$^+$-pillared bentonite: isotherm, kinetic and thermodynamic aspects, J. Radioanal. Nucl. Chem., 293 (2012) 231–239.

[13] A.S. Özcan, Ö. Gök, A. Özcan, Adsorption of lead(II) ions onto 8-hydroxy quinoline-immobilized bentonite, J. Hazard. Mater., 161 (2009) 499–509.

[14] J. Su, H. Huang, X. Jin, X. Lu, Z. Chen, Synthesis, characterization and kinetic of a surfactant-modified bentonite used to remove As(III) and As(V) from aqueous solution, J. Hazard. Mater., 185 (2011) 63–70.

[15] L.A. Shah, M. das G. da Silva Valenzuela, M. Farooq, S.A. Khattak, F.R. Valenzuela Díaz, Influence of preparation methods on textural properties of purified bentonite, Appl. Clay Sci., 162 (2018) 155–164.

[16] J. Ma, J. Qi, C. Yao, B. Cui, T. Zhang, D. Li, A novel bentonite-based adsorbent for anionic pollutant removal from water, Chem. Eng. J., 200–202 (2012) 97–103.

[17] S. Pandey, J. Ramontja, Recent modifications of bentonite clay for adsorption applications, Focus Sci., 2 (2016) 1–10.

[18] A. Bentouami, M.S. Ouali, Cadmium removal from aqueous solutions by hydroxy-8 quinoline intercalated bentonite, J. Colloid Interface Sci., 293 (2006) 270–277.

[19] Ö. Gök, A. Özcan, B. Erdem, A.S. Özcan, Prediction of the kinetics, equilibrium and thermodynamic parameters of adsorption of copper(II) ions onto 8-hydroxy quinoline immobilized bentonite, Colloids Surf., A, 317 (2008) 174–185.

[20] G. Kahr, F.T. Madsen, Determination of the cation exchange capacity and the surface area of bentonite, illite and kaolinite by methylene blue adsorption, Appl. Clay Sci., 9 (1995) 327–336.

[21] S.A. Marczenko, Separation and Spectrophotometric Determination of Elements, Hoboken, John Wiley, NJ, USA, 1986, pp. 424–446.

[22] E. Bentouhami, G.M. Bouet, J. Meullemeestre, F. Vierling, M.A. Khan, Physicochemical study of the hydrolysis of rare-earth elements (III) and thorium(IV), C.R. Chim., 7 (2004) 537–545.

[23] B.A. Salah, M.S. Gaber, A.T. Kandil, The removal of uranium and thorium from their aqueous solutions by 8-hydroxyquinoline immobilized bentonite, Minerals, 9 (2019) 626, doi: 10.3390/min9100626.

[24] A. Sheikhmohammadi, S.M. Mohseni, R. Khodadadi, M. Sardar, M. Abtahi, S. Mahdavi, H. Keramati, Z. Dahaghin, S. Rezaei, M. Almasian, M. Sarkhosh, M. Faraji, S. Nazari, Application of graphene oxide modified with 8-hydroxyquinoline for the adsorption of Cr(VI) from wastewater: optimization, kinetic, thermodynamic and equilibrium studies, J. Mol. Liq., 233 (2017) 75–88.

[25] Y.Q. Wang, Z. Bin Zhang, Q. Li, Y.H. Liu, Adsorption of thorium from aqueous solution by HDTMA$^+$-pillared bentonite, J. Radioanal. Nucl. Chem., 293 (2012) 519–528.

[26] S.S. Dubey, S. Grandhi, Sorption studies of yttrium(III) ions on surfaces of nano-thorium(IV) oxide and nano-zirconium(IV) oxide, Int. J. Environ. Sci. Technol., 16 (2019) 59–70.

[27] G. Wójcik, Sorption behaviors of light lanthanides(III) (La(III), Ce(III), Pr(III), Nd(III)) and Cr(III) using nitrolite, Materials (Basel), 13 (2020) 2256, doi: 10.3390/ma13102256.

[28] S.U. Aja, Sorption of the rare earth element, Nd, onto kaolinite at 25°C, Clays Clay Miner., 46 (1998) 103–109.

[29] P. Sappidi, A. Boda, S.M. Ali, J.K. Singh, Adsorption of gadolinium ($Gd^{3+}$) ions on the dibenzo crown ether (DBCE) and dicyclo hexano crown ether (DCHCE) grafted on the polystyrene surface: insights from all atom molecular dynamics simulations and experiments, J. Phys. Chem. C, 123 (2019) 12276–12285.

[30] Z.Y. Bunina, K. Bryleva, O. Yurchenko, K. Belikov, Sorption materials based on ethylene glycol dimethacrylate and methacrylic acid copolymers for rare earth elements extraction from aqueous solutions, Adsorpt. Sci. Technol., 35 (2017) 545–559.

[31] D. Li, X. Chang, Z. Hu, Q. Wang, R. Li, X. Chai, Samarium(III) adsorption on bentonite modified with N-(2-hydroxyethyl) ethylenediamine, Talanta, 83 (2011) 1742–1747.

[32] S.H. Dubey, S. Grandhi, Optimization of samarium(III) sorption using nano-zirconium oxide by Taguchi Method SOM, Asian J. Chem., 30 (2018) 1717–1722.